

See discussions, stats, and author profiles for this publication at: <https://www.researchgate.net/publication/45706424>

# Quasi-Confocal, Multichannel Parallel Scan Hyperspectral Fluorescence Imaging Method Optimized for Analysis of Multicolor Microarrays

ARTICLE *in* ANALYTICAL CHEMISTRY · SEPTEMBER 2010

Impact Factor: 5.64 · DOI: 10.1021/ac101629x · Source: PubMed

---

CITATIONS

14

---

READS

27

8 AUTHORS, INCLUDING:



Zhiyi Liu

Tsinghua University

27 PUBLICATIONS 129 CITATIONS

SEE PROFILE



Le Liu

Tsinghua University

55 PUBLICATIONS 293 CITATIONS

SEE PROFILE



Hui Ma

Tsinghua University

117 PUBLICATIONS 782 CITATIONS

SEE PROFILE

# Quasi-Confocal, Multichannel Parallel Scan Hyperspectral Fluorescence Imaging Method Optimized for Analysis of Multicolor Microarrays

Zhiyi Liu,<sup>†</sup> Suihua Ma,<sup>†</sup> Yanhong Ji,<sup>\*,‡</sup> Le Liu,<sup>†</sup> Zhaoxu Hu,<sup>†</sup> Jihua Guo,<sup>†</sup> Hui Ma,<sup>†</sup> and Yonghong He<sup>\*,†</sup>

Laboratory of Optical Imaging and Sensing, Graduate School at Shenzhen, Tsinghua University, Shenzhen, 518055, P. R. China, and MOE Key Laboratory of Laser Life Science and Institute of Laser Life Science, South China Normal University, Guangzhou, 510631, P. R. China

The microarray technique, which can provide parallel detection with high throughput in biomedical research, has generated considerable interest since the end of the 20<sup>th</sup> century. A number of instruments have been reported for microarray detection. In this paper, we have developed a quasi-confocal, multichannel parallel scan hyperspectral fluorescence imaging system for multicolor microarray research. Hyperspectral imaging records the entire emission spectrum for every voxel within the imaged area in contrast to recording only fluorescence intensities of filter-based scanners. When coupled with data analysis, the recorded spectral information allows for quantitative identification of the contributions of multiple, spectrally overlapping fluorescent dyes and elimination of unwanted artifacts. This system is improved with a specifically designed, high performance spectrometer which can offer a spectral resolution of 0.2 nm and operates with spatial resolutions ranging from 2 to 30  $\mu\text{m}$ . We demonstrate the application of the system by reading out arrays for identification of bacteria.

The advent of DNA microarrays has revolutionized the biomedical research in genetic engineering.<sup>1,2</sup> A DNA microarray is a two-dimensional array of genetic elements immobilized on a solid surface. For a typical microarray, tens of thousands of spots with the order of  $\sim 100 \mu\text{m}$  are printed on the substrate, leading to a greatly improved experimental throughput.<sup>3–7</sup> Microarray research, which offers great potential for analysis of gene expression profile, has been an advanced technology for biomedical applications.

Although microarray technology is of growing importance in various fields of research, such as genomics, proteomics, pharmaceuticals, and medical diagnostics, it is still young and in need of improvement in many aspects. The detection method for

microarrays is of interest in the current study. A number of methods have been developed, such as chemiluminescence,<sup>8</sup> surface plasmon resonance,<sup>9,10</sup> and fluorescence markers.<sup>11</sup> Fluorescence imaging is popular for the readout of microarrays. Most fluorescence scanners detect the band-integrated emission corresponding to the band-pass filter utilized for each fluorophore.<sup>12–14</sup> In these scanners, one filter corresponds to one kind of fluorophore. This approach is a direct imaging of sample plane; however, there are some drawbacks in this measurement approach. First, as different fluorescent tags are excited with different wavelengths and the fluorescence signals are distinguished by band-pass filters, the chosen fluorescent tags should have minimal overlap of their emission spectra. Second, for these filter-based scanners, it is difficult to determine whether the measured data have been corrupted by some extraneous emission sources. For example, the spot-localized contamination due to spotting chemistry and the emission from substrates<sup>15</sup> affect the determination of gene expression, especially for weakly expressed genes. These drawbacks, aforementioned, limit this approach in reliable and high-accuracy analysis of microarrays.

Hyperspectral imaging overcomes these limitations by recording the entire emission spectrum for every voxel within the imaged area in contrast to recording only fluorescence intensities of filter-

- (3) Cheung, V. C.; Morley, M.; Aquilar, F.; Massimi, A.; Kucherlapati, R.; Childs, G. *Nat. Genet.* **1999**, *21* (Suppl.), 15–19.
- (4) Van Hal, N. L. W.; Vorst, O.; Van Houwelingen, A. M. M. L.; Kok, E. J.; Peijnenburg, A.; Aharoni, A.; Van Tunen, A. J. *J. Biotechnol.* **2000**, *78*, 271–280.
- (5) Duggan, D. J.; Bittner, M.; Chen, Y.; Meltzer, P.; Trent, J. M. *Nat. Genet.* **1999**, *21* (Suppl.), 10–14.
- (6) Brown, P. O.; Botstein, D. *Nat. Genet.* **1999**, *21*, 33–37.
- (7) Huang, Y.; Joo, S.; Duhon, M.; Heller, M.; Wallace, B.; Xu, X. *Anal. Chem.* **2002**, *74*, 3362–3371.
- (8) Wolter, A.; Niessner, R.; Seidel, M. *Anal. Chem.* **2008**, *80*, 5854–5863.
- (9) Homola, J. *Chem. Rev.* **2008**, *108*, 462–493.
- (10) Liu, L.; He, Y.; Zhang, Y.; Ma, S.; Ma, H.; Guo, J. *Appl. Opt.* **2008**, *47*, 5616–5621.
- (11) Moczko, E.; Meglinski, I. V.; Bessant, C.; Piletsky, S. A. *Anal. Chem.* **2009**, *81*, 2311–2316.
- (12) Ruckstuhl, T.; Walser, A.; Verdes, D.; Seeger, S. *Biosens. Bioelectron.* **2005**, *20*, 1872–1877.
- (13) Huang, G. L.; Deng, C.; Zhu, J.; Xu, S. K.; Han, C.; Song, X. B.; Yang, X. Y. *J. Biomed. Opt.* **2008**, *13*, 034006.
- (14) Liu, Z.; He, Y.; Liu, L.; Ma, S.; Chong, X.; Hu, Z.; Ma, H.; Guo, J. *Opt. Lasers Eng.* **2010**, *48*, 849–855.
- (15) Martinez, M. J.; Aragon, A. D.; Rodriguez, A. L.; Weber, J. M.; Timlin, J. A.; Sinclair, M. B.; Haaland, D. M.; Werner-Washburne, M. *Nucleic Acids Res.* **2003**, *31*, e18.

\* Corresponding author. E-mail: heyh@sz.tsinghua.edu.cn (Y.H.); jiyh@snu.edu.cn (Y.J.).

<sup>†</sup> Tsinghua University.

<sup>‡</sup> South China Normal University.

(1) Fodor, S. P.; Read, J. L.; Pirrung, M. C.; Stryer, L.; Lu, A. T.; Solas, D. *Science* **1991**, *251*, 767–773.

(2) Fodor, S. P.; Rava, R. P.; Huang, X. C.; Pease, A. C.; Holmes, C. P.; Adams, C. L. *Nature* **1993**, *364*, 555–556.

based scanners. Multivariate data exploitation, which is able to accurately determine the concentrations of different emission sources, is then used for analysis of spectral information.<sup>16,17</sup> Thus, hyperspectral imaging is able to identify multiple fluorescent tags with a single wavelength within a single scan and eliminate unwanted artifacts described above. Moreover, hyperspectral scanning permits minimal use of optical filters for analysis of multicolor microarrays due to recording of spectra, thus offering advantages over filter-based scanners. The wealth of information that is available from spectrally resolving an image makes hyperspectral imaging an extremely attractive technique, and various hyperspectral instruments have been reported over the past years.<sup>18–23</sup> In these papers, hyperspectral fluorescence imaging systems are employed mainly for imaging biological samples, and some efforts have been devoted to microarray research, while we attempt to develop a system further improved and optimized for microarray readout.

We have previously developed a quasi-confocal parallel scan fluorescence imaging system, which is a filter-based scanner for analysis of microarrays.<sup>14</sup> Different from laser confocal scanners which are point-focusing of the laser light, the quasi-confocal method focuses the laser light to a line, and the whole region of interest is detected with parallel scan of the line light along the direction vertical to the line. The quasi-confocal method acquires images with nearly the same performance as the strict confocal images provided by a flying-spot scanning method,<sup>24</sup> and parallel scan offers a high throughput which is important for microarray analysis. Considering the advantages offered by quasi-confocal parallel scan architecture and the great potential of hyperspectral imaging, in this paper, we improve the former system and develop a quasi-confocal, multichannel parallel scan hyperspectral method for analysis of microarrays. In order to identify highly overlapping fluorescent dyes which are popular as labels, this system is improved with a specifically designed, high-performance spectrometer, which can provide a high effective spectral resolution and adequate spectral range. Two lasers are presently employed to cover different spectral regions, and new lasers could be easily added as light sources due to the optical design of the system, thus offering a multichannel imaging covering large spectral

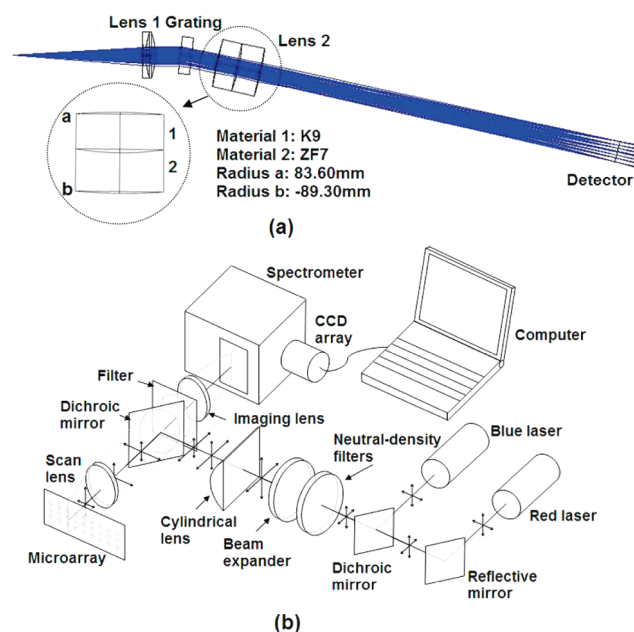


**Figure 1.** Optical design of the system. (a) Spectrometer design. (b) Layout of the system.

ranges. The spatial resolution, reproducibility, and sensitivity of this system are discussed in detail. Finally, the application of the system is demonstrated by reading arrays for identification of bacteria.

## METHODS AND MATERIALS

**Spectrometer Design.** At present, fluorescent dye sets used in multicolor microarray genotyping usually contain mixtures of chemically and structurally different dyes, such as fluoresceins, rhodamines, and cyanines.<sup>25–27</sup> For example, Cyanine 5 (Cy5) and naphthofluorescein (Nap) are popular as fluorescent tags corresponding to red laser excitation. The spectra of these two dyes are highly overlapping, with only 3 nm difference in wavelength at maximum fluorescence intensities. Thus, a spectrometer with a high spectral resolution, not at the expense of spectral range, is needed for discrimination of highly overlapping fluorescent dyes.

Figure 1a shows a Zemax model of the homemade spectrometer based on the transmission grating and achromatic lenses.<sup>28</sup> Lens 1 is an achromatic lens with the focus length of 70 mm. A transmission grating with the size of  $25 \times 25 \text{ mm}^2$  is used as the dispersion optics. The density of the grating is 300 lines/mm, which is selected considering both the spectral range of the fluorescent tags and the spectral resolution. Lens 2 is important to optical properties of the spectrometer; thus, lens 2 is designed and modified repeatedly for minimum aberration. The focus length of lens 2 is 200 mm, and design parameters of lens 2, including materials and surface curvature radii, are listed in Figure 1a. The detector has  $4752 \times 3168$  pixels with  $4.7 \times 4.7 \mu\text{m}^2$  per pixel.

The orientation of the grating is determined by eq 1 as follows:

$$d(\sin \theta + \sin \varphi) = \lambda_u \quad (1)$$

where  $d$  is the grating constant,  $\theta$  is the angle between lens 1 and grating,  $\varphi$  is the angle between grating and lens 2, and  $\lambda_u$  is

(28) Hu, Z.; Rollins, A. M. *Proc. SPIE* **2007**, 6429, 642925.

- (16) Haaland, D. M.; Sinclair, M. B.; Timlin, J. A.; Van Benthem, M. H.; Martinez, M. J.; Aragon, A. D.; Werner-Washburne, M. *Proc. SPIE* **2003**, 4959, 55–67.
- (17) Bro, R.; DeJong, S. J. *Chemom.* **1997**, 11, 393–401.
- (18) Erfurth, F.; Tretjakov, A.; Nyuyki, B.; Mrotzek, G.; Schmidt, W. D.; Fassler, D.; Saluz, H. P. *Anal. Chem.* **2008**, 80, 7706–7713.
- (19) Schultz, R. A.; Nielsen, T.; Zavaleta, J. R.; Ruch, R.; Wyatt, R.; Garner, H. R. *Cytometry* **2001**, 43, 239–247.
- (20) Sinclair, M. B.; Haaland, D. M.; Timlin, J. A.; Jones, H. D. T. *Appl. Opt.* **2006**, 45, 6283–6291.
- (21) Tsurui, H.; Nishimura, H.; Hattori, S.; Hirose, S.; Okumura, K.; Shirai, T. *J. Histochem. Cytochem.* **2000**, 48, 653–662.
- (22) Sinclair, M. B.; Timlin, J. A.; Haaland, D. M.; Werner-Washburne, M. *Appl. Opt.* **2004**, 43, 2079–2088.
- (23) Stimson, M. J.; Haralampus-Grynaviski, N.; Simon, J. D. *Rev. Sci. Instrum.* **1999**, 70, 3351–3354.
- (24) Hammer, D. X.; Ferguson, R. D.; Ustun, T. E.; Bigelow, C. E.; Iftimia, N. V.; Webb, R. H. J. *Biomed. Opt.* **2006**, 11, 041126.
- (25) Hirschhorn, J. N.; Sklar, P.; Lindblad-Toh, K.; Lim, Y. M.; Ruiz-Gutierrez, M.; Bolk, S.; Langhorst, B.; Schaffner, S.; Winchester, E.; Lander, E. S. *Proc. Natl. Acad. Sci. U.S.A.* **2000**, 97, 12164–12169.
- (26) Lindroos, K.; Sigurdsson, S.; Johansson, K.; Ronnblom, L.; Syvanen, A. C. *Nucleic Acids Res.* **2002**, 30, e70.
- (27) Kurg, A.; Tonisson, N.; Georgiou, I.; Shumaker, J.; Tollett, J.; Metspalu, A. *Genet. Test.* **2000**, 4, 1–7.

the center wavelength of the fluorescence emission. In our system, a red laser and a blue laser are utilized as light sources for the excitation of fluorescence.  $\lambda_{\text{u}}$  is 730 nm, corresponding to red laser excitation, and 540 nm, corresponding to blue laser excitation, respectively. When the laser is changed from one to the other, only an easy change of grating orientation is needed for two-channel detection.

This spectrometer has an effective spectral resolution (fwhm) of 0.2 nm, compared with  $\sim 1$  nm of common commercial spectrometers, and covers more than a 200 nm spectral range corresponding to each laser. This spectrometer is a straightforward design with high performance optimized for microarray scanning.

**Constitution of the Hyperspectral Scanner.** Figure 1b shows the optical layout of the system. A He–Ne laser with a wavelength of 632.8 nm and a power of 12.5 mW and a solid state laser with a wavelength of 473 nm and a power of 12.5 mW are used as light sources. Two lasers are present here; however, new lasers could be easily added to the system to enlarge spectral ranges for multichannel detection. The laser fluence is adjusted to fit experimental conditions by the use of a filter wheel populated with a set of neutral-density filters. The laser light is broadened by a beam expander and directed through a cylindrical lens ( $f = 30$  mm) for the desired line illumination. Then, a dichroic mirror, which is characterized by high reflectivity at the laser wavelength and high transparency at longer wavelengths, is used to direct the laser light through the scan lens ( $f = 50$  mm). For higher resolution and fluorescence collection efficiencies, apochromatic objectives with high numerical apertures (NA) are used.

The line length of the focused laser light is approximately 5 mm on the surface of the microarray. The array is mounted on the scan stage, which is capable of 80 mm of travel in the  $x$  direction and 60 mm of travel in the  $y$  direction. Fluorescence excited by the focused line light is collected by the scan lens and directed through the dichroic mirror. A band-pass filter is used to further eliminate unwanted scattered and reflected laser light. An imaging lens ( $f = 80$  mm) is then used to focus the fluorescence signals for a line image, which is relayed to the entrance slit of the spectrometer for the acquisition of the spectrally dispersed image. A CCD array (Canon 500D) records these spectrally dispersed images for further data analysis. Then, the whole plane is detected with parallel scan along the direction vertical to the focused line. The system achieves so-called “quasi-confocal” imaging because some light from adjacent voxels along the illuminated line could mix at the CCD array. While vertical to the illuminated line, light from adjacent voxels is efficiently rejected.

**Fabrication of Microarrays.** Throughout this study, we prepare microarrays ourselves to test the characterization and the imaging capability of the system. For the fabrication of the DNA arrays, the magnetron sputtering gold films are used as substrates. The fluorophores labeled DNA strands are thiolated for covalent bonding to substrates. Cy5 (absorption/emission: 649/667 nm) and Dylight 680 (absorption/emission: 680/715 nm) are employed as fluorescent tags corresponding to the red laser. Bodipy 493/503 (absorption/emission: 500/506 nm) and rhodamine green (absorption/emission: 504/533 nm) are used corresponding to the blue laser.

The gold film needs to be cleaned thoroughly before the printing of sample spots. First, the gold film is cleaned with a

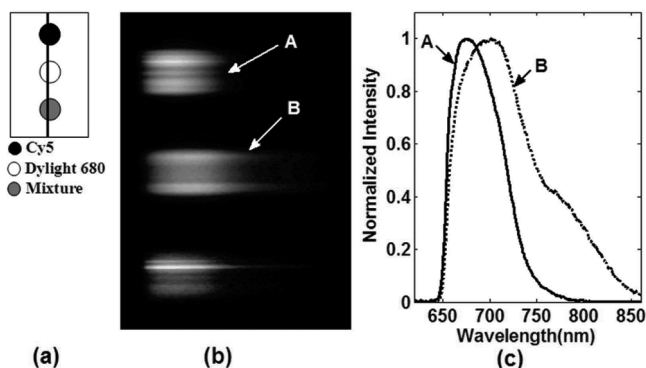


**Figure 2.** Hyperspectral data analysis. (a) Design of the dye labeled spots. (b) A single frame of data corresponding to the line in (a). (c) Intensity curves of rows marked in (b).

solution consisting of  $\text{H}_2\text{O}_2$  (30%),  $\text{NH}_3$  (30%), and deionized water in a 1:1:5 ratio for 10 min.<sup>29</sup> Then, the film is dipped into acetone and ethanol for 10 min oscillating successively. After that, the film is thoroughly rinsed by deionized water and then dried and stored until further use.

The fluorescence labeled DNA is dissolved with ultra pure water to prepare solutions with different concentrations. When all above are ready, the gold film is put into a wet box, which provides a wet environment for the whole process of array printing. In our study, printing of the array is carried out manually. After that, the gold film, kept in the wet box, is put into the electric heating constant temperature incubator (Shanghai Permanent Science and Technology the Limited company, DHP-9052) for a 2 h incubation at 37 °C. Then, the DNA array is ready for optical scan.

Equation 2 shows the calculation of sample density ( $D_s$ ) for the printed spots:

$$D_s = V_p \times M_p \times N_A / A_o \quad (2)$$

where  $N_A$  is the Avogadro's constant,  $V_p$  is the extracted volume for one spot,  $M_p$  is the concentration of fluorescent dye with the unit of  $\mu\text{mol/L}$ , and  $A_o$  is the area of one spot on the sensing plane. Thus, the unit of sample density is the number of fluorescence molecules per square micrometer ( $\text{fluors}/\mu\text{m}^2$ ). The spots with variant sample densities can be acquired by adjusting concentrations of fluorescent dye.

**Hyperspectral Data Analysis.** Analysis of hyperspectral data is crucial to the fluorescence image reconstruction and gene expression. Prior to analysis of the hyperspectral data, calibration data frames of the system are obtained by use of mercury argon calibration source (Ocean Optics). The acquired spectral data can be used to calibrate the wavelength scale and remove the slight influence of image curvature due to the spectrometer with the linear interpolation method.

To illustrate the hyperspectral data analysis, a sensing model of manually printed sample spots is prepared, as shown in Figure 2a. Figure 2b shows one frame of data corresponding to the vertical line in Figure 2a. Each row represents the spectrum of one certain point in the line region; thus, the entire picture of Figure 2b is the spectra of illuminated line region. Figure 2c shows

(29) Wang, R. H.; Sara, T.; Maria, M.; Maria, M. S.; Marco, M. *Biosens. Bioelectron.* **2004**, *20*, 967–974.



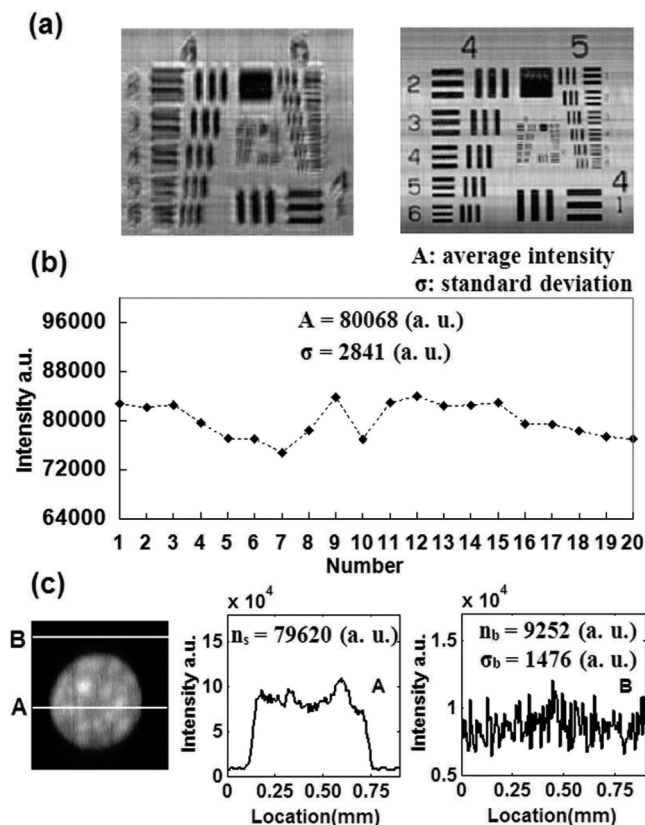


**Figure 3.** Spatial resolution, reproducibility, and sensitivity of the system. (a) Scanning images of the standard resolution target. Left: 30  $\mu\text{m}$  resolution; right: 10  $\mu\text{m}$  resolution. (b) Signal intensities of spots in 20 experiments. A is the average intensity of these spots;  $\sigma$  is the standard deviation of the recorded intensities. (c) Left: the scanning image of a spot; middle and right: intensity graphs of the marked rows A and B, respectively. The values of  $n_s$ ,  $n_b$ , and  $\sigma_b$  are given in the graphs.

the intensity curves of the rows marked in Figure 2b, which are normalized for comparison. As can be seen from Figure 2c, the normalized spectra of these two dyes are overlapped. The spectra of the points within mixture spots depend on the concentration ratios of these two dyes. Multivariate data analysis is used to determine the concentrations of different emission sources, which will be demonstrated in detail in Multichannel Fluorescence Imaging. For every voxel on the array plane, the intensity of each emission source is calculated by integration of the corresponding spectrum. The whole image of the array is acquired by analysis of all the data frames obtained during optical scan.

## SYSTEM CHARACTERIZATION

**Performance of the Hyperspectral Scanner.** The spatial resolution of this hyperspectral system is characterized using a U.S. Air Force standard resolution target (Edmund Optics) with broadband illumination. As mentioned above, this system is designed to enable simple changes of scan lens to obtain different resolutions for variant applications. Figure 3a (left) is an image of the resolution target obtained by an achromatic lens with the focus length of 50 mm. As can be seen from this image, element 1 of group 4 of the resolution target, corresponding to 16.0 line pairs/mm ( $\sim 31 \mu\text{m}$ ), is resolved in both the horizontal and the vertical direction. For higher resolution, a 10 $\times$ , NA 0.25 objective is also available, and the corresponding

image is shown in Figure 3a (right). In this case, element 4 of group 5, corresponding to 45.3 line pairs/mm ( $\sim 11 \mu\text{m}$ ), can be resolved. The spot diameters and center-to-center spacings of commercial microarrays are on the order of  $\sim 100 \mu\text{m}$ ; thus, the 10–30  $\mu\text{m}$  resolution is good and adequate for microarray analysis. A 40 $\times$ , NA 0.65 objective is used for an even higher resolution of  $\sim 2 \mu\text{m}$  and higher fluorescence collecting efficiencies than the 10 $\times$  objective. Thus, the resolution of this hyperspectral system ranges from 2 to 30  $\mu\text{m}$ . However, as the length of the scan line, corresponding to the throughput within a single scan, decreases with the use of high magnification objectives, we should choose the spatial resolution according to the size of the array.

Then, experiments are carried out to test the reproducibility of the system. We prepare the Cy5-DNA array with only one spot corresponding to a sample density of 30 fluors/ $\mu\text{m}^2$  and, then, make an imaging of the array with our system. We repeat this “array fabrication-imaging” process 20 times and record the intensity of each spot, as shown in Figure 3b. The average intensity of these spots is 80068 (a. u.), with a standard deviation of 2841 (a. u.); thus, a fluctuation is as low as 3.5% in 20 experiments.

The sensitivity of fluorescence imaging is calculated as follows:<sup>30,31</sup>

$$S_d = D_s / \text{SNR} \quad (3)$$

$$\text{SNR} = (n_s - n_b) / \sigma_b \quad (4)$$

where  $S_d$  is the detection sensitivity,  $D_s$  is the sample density, and SNR is the signal-to-noise ratio. Equation 4 shows the calculation of SNR,<sup>32</sup> where  $n_s$  is the average intensity obtained from the spot of interest,  $n_b$  is the average intensity of background, and  $\sigma_b$  is the standard deviation of background. We use one frame of the 20 images acquired in the reproducibility experiment for illustration, as shown in Figure 3c (left); thus, the sample density of this spot is 30 fluors/ $\mu\text{m}^2$ . To demonstrate the signal intensity and background noise level, intensity graphs of the marked rows A and B are plotted to the right of the spot image, and the values of  $n_s$ ,  $n_b$ , and  $\sigma_b$  are given in the graphs. Calculated by eq 4, an SNR of approximately 48 is derived; thus, the detection sensitivity is 0.63 fluors/ $\mu\text{m}^2$  according to eq 3. The sensitivity can be further improved by the pixel binning method.<sup>14</sup> The sensitivity achieved from this hyperspectral fluorescence imaging system is comparable to that of commercial microarray scanners; thus, it is adequate for analysis of most microarrays.

To test the imaging capability of the system, a sensing model of a 10  $\times$  5 Cy5-DNA array is prepared. For all spots of a column, the same sample density is applied; some sample densities recur in different columns. The densities are 2, 4, 6, 8, and 10 fluors/ $\mu\text{m}^2$  from the left side. Figure 4a shows the scanning image of the sensing model. The shape and detail of these spots are clearly observed, and the fluorescence intensity of the spots increases

(30) Nicolini, C.; Malvezzi, A. M.; Tomaselli, A.; Sposito, D.; Tropiano, G.; Borgogno, E. *IEEE Trans. Nanobiosci.* **2002**, *1*, 67–72.

(31) Nagarajan, R.; Peterson, C. A. *IEEE Trans. Nanobiosci.* **2002**, *1*, 78–84.

(32) Schena, M. *Microarray Biochip Technology*; Eaton Publishing: Natick, MA, 2000.

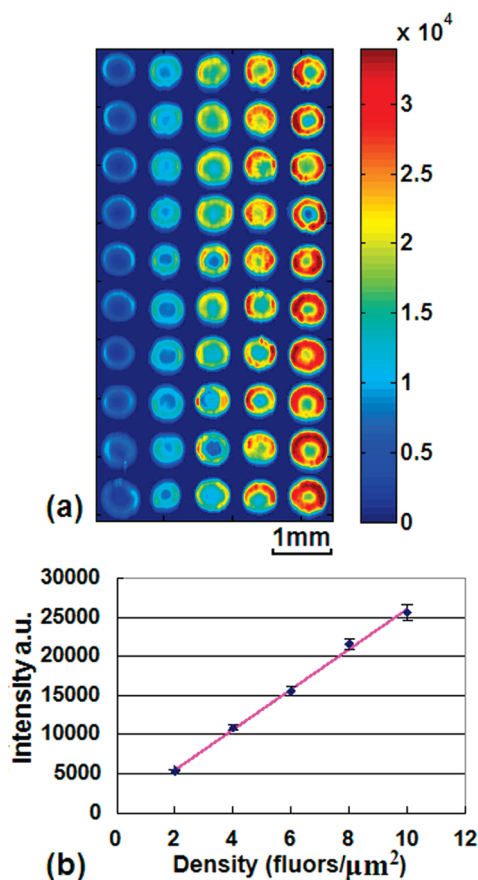


**Figure 4.** Relationship between fluorescence intensity and sample density. (a) Image of a  $10 \times 5$  DNA-array. (b) Plot of fluorescence intensity against Cy5 density. The points represent the average fluorescence intensity of the columns, and the error bars give the deviation within one column.

with the increasing sample density. Figure 4b depicts the average spot intensity of each column against the sample density. As expected, there is a linear dependence of fluorescence signal on the sample density, while the data points scatter around the linear fit. The excitation intensity is reduced by neutral-density filters, and the exposure time is adjusted to syntonize the fluorescence signal to the sensing range of the detector. Moreover, the error bars for each sample density are offered in Figure 4b, illustrating the deviation within one column.

**Multichannel Fluorescence Imaging.** To investigate the multichannel, hyperspectral imaging performance of the system, sensing models were designed for optical scan. In Figure 5a, both dyes of Bodipy 493/503 and rhodamine green, corresponding to the blue laser and overlapping in spectra, are applied to fabricate a microarray. In this array, each spot contains only a single type of fluorescent dye, and the distributions of the tags are demonstrated in Figure 5a. This case corresponds to the multicolor labeling strategy which is generally utilized in gene expression research.<sup>33</sup> The two-dimensional image of this array is shown in Figure 5b. The colors of brown and green are utilized to represent the dyes of Bodipy 493/503 and rhodamine green, respectively. The raw spectra of the pixels pointed by the arrows are shown in Figure 5c. For presentation, only two dyes are applied here corresponding to a single laser; the scanning image demonstrates

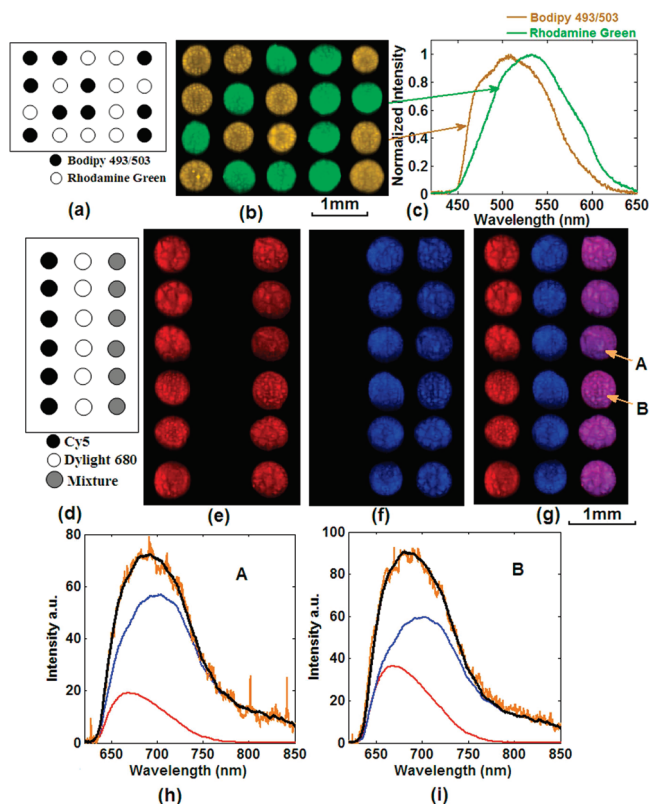


**Figure 5.** Hyperspectral imaging of spectrally overlapping fluorescent dyes. (a) Design of an array with spots containing DNA strands labeled with a single dye. (b) Scanning image of the array in (a). (c) Normalized spectra of the labeled dyes. (d) Design of an array with different kinds of spots. (e) Image of Cy5. (f) Image of Dylight 680. (g) Image of the whole sample plane. (h) and (i) Multivariate data analysis for the determination of the ratios of each dye. Red curve: the weighted spectrum for Cy5; blue curve: the weighted spectrum for Dylight 680; brown curve: the raw spectrum for a certain point of the mixture spots; black curve: the calculated spectrum as a sum of these two weighted spectra.

the ability of this hyperspectral scanner to identify multiple fluorescent labels with spectral analysis.

We have demonstrated the capability of this system to image the spots containing DNA strands labeled with a single dye, which are used to mimicking homozygotes in multicolor genotyping microarray experiments. In order to mimic heterozygotes<sup>27,34</sup> and eliminate unwanted artifacts, such as emission from substrates and spot-localized contamination, a more demanding test to analyze spots labeled with multiple dyes is carried out. We design a sensing model for demonstration, as shown in Figure 5d. For all the spots in the first column, only Cy5 labeled DNA is used, and only Dylight 680 labeled DNA is applied in the second column. For all the spots in the third column, a mixture of these two dyes is applied. Figure 5e,f shows the fluorescence images of Cy5 and Dylight 680, respectively. The whole image of the sample plane is acquired by combining the concentration maps of these two dyes, as shown in Figure 5g. The raw emission spectra (brown color) for two points A and B in Figure 5g are shown in Figure 5h,i. Although the same Cy5-Dylight 680 ratio is applied for spots in the third column, the spectra of the points within one spot vary

(33) Bender, K. *Methods Mol. Biol.* **2005**, *297*, 243–252.

(34) Lovmar, L.; Ahlford, A.; Jonsson, M.; Syvanen, A. C. *BMC Genomics* **2005**, *6*, 35.

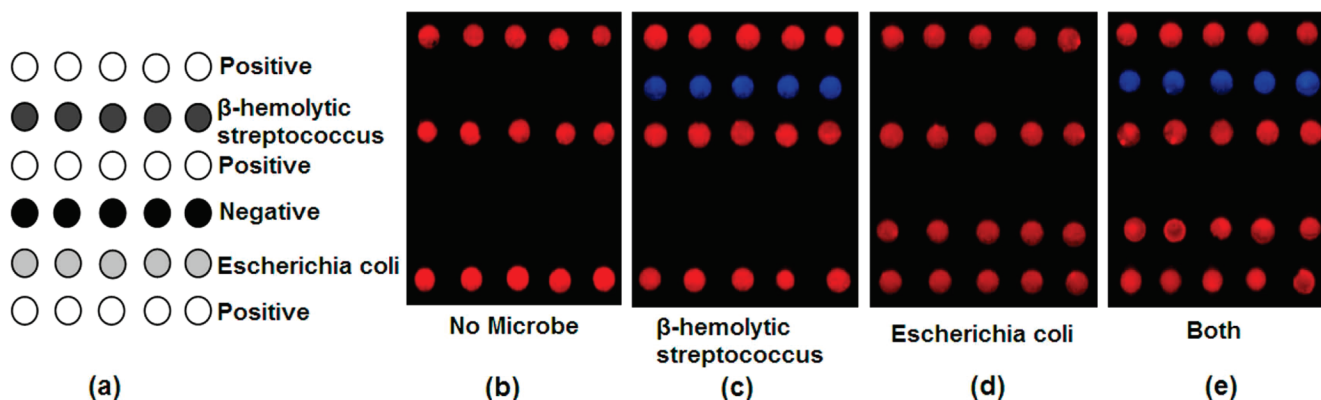


**Figure 6.** Identification of bacteria as an example of biomedical application of microarrays. (a) Design of the microarray. Scanning results with (b) no microbe, (c) only *β*-hemolytic streptococcus, (d) only *Escherichia coli*, and (e) both two microbes in the sample.

from each other due to the inhomogeneities of distributions of fluorescence molecules. With multivariate data analysis, the weight of each dye is determined. In Figure 5h,i, the red and blue curves correspond to the weighted spectra of Cy5 and Dylight 680, respectively, and the black curve is a sum of these two weighted spectra. As can be seen from Figure 5h,i, the sum curves (black) correspond well to the raw spectra (brown) of the two randomly chosen points, indicating that the entire hyperspectral image stack could be modeled using linear admixtures of these two dyes. The scanning results demonstrate that discrimination of multiple emissions overlapped spatially does not present a difficulty for the hyperspectral system.

## BIOMEDICAL APPLICATION OF MICROARRAYS

The identification of bacteria using gene chips is performed by this quasi-confocal, parallel scan hyperspectral fluorescence imaging system as an example of biomedical application of microarrays.

A gold film covered quartz glass is used as the substrate, which is carefully cleaned before the printing of probes. Then, four  $6 \times 5$  probe arrays are printed manually on the substrates. All the probes are thiolated for covalent bonding to gold films. As shown in Figure 6a, the array comprises one row of *Escherichia coli* probes, one row of *β*-hemolytic streptococcus probes, one row of negative probes as quality report marks of the chip hybridization, and three rows of positive probes. For the validation of results on the chip, the positive probes should show a high fluorescent intensity signal, and the negative probes should show a low (or zero) signal.

Throughout this study, Cy5 is used for positive and *Escherichia coli* DNA fragments, and Dylight 680 is for *β*-hemolytic streptococcus. Figure 6b shows the detection results with no microbe present in the sample. As expected, the positive probes report a high fluorescent intensity signal, while the negative probes show a blank signal. If *β*-hemolytic streptococcus is present in a sample, then the row of *β*-hemolytic streptococcus probes will show a high signal. Similarly, the row of *Escherichia coli* probes will show a high signal if *Escherichia coli* is present in a sample. Figure 6c,d shows the experimental results corresponding with expectation. Figure 6e is the detection results with both *β*-hemolytic streptococcus and *Escherichia coli* present in the sample, and all the rows, except the row of negative probes, show a high signal. The experimental results indicate that the target genes are selectively

hybridized to the probes. This hyperspectral system generates high quality images and can be successfully applied in biomedical research.

## CONCLUSIONS

In this paper, we have proposed a quasi-confocal, multichannel parallel scan hyperspectral fluorescence imaging system. This system employs a pushbroom scan architecture with the line focusing of the excitation laser and records the spectrum for every voxel of the excited line region, and the whole sample plane is detected with parallel scan vertical to the scanning line. For hyperspectral imaging, the spectral resolution is important to the spectra identification and, then, the accurate determination of gene expression ratios; thus, we design and construct a spectrometer which offers a high spectral resolution of 0.2 nm and a spectral range more than 200 nm corresponding to each laser. As a result, this system is able to identify highly overlapping dyes, e.g., Cy5 and Nap, with only 3 nm difference in wavelength at maximum fluorescence intensities, and the 0.2 nm resolution is adequate for discrimination of most commercially available fluorescent labels. Coupled with multivariate data analysis, this system is capable of quantitative analysis of the concentrations of all the emitting species for any pixel on the sample plane. The spatial resolution of this system ranges from 2 to 30  $\mu\text{m}$ . Although the quasi-confocal mechanism limits the system in extreme high-resolution microscopic imaging, the spatial resolution of this system is particularly suitable for imaging of microarrays. This system offers a sensitivity of 0.63 fluors/ $\mu\text{m}^2$ , which is adequate and good for microarray analysis. The application of this system is demonstrated by reading multicolor microarrays for identification of bacteria. We believe that the proposed hyperspectral system can be used to build a commercially valuable device for microarray analysis application.

## ACKNOWLEDGMENT

This research was made possible with the financial support from the 863 project, China (Grant 2006AA06Z402), and NSFC China (Grants 30770592 and 60608019).

Received for review June 21, 2010. Accepted August 6, 2010.

AC101629X